Mid-Late Holocene vegetation and hydrological variations in Songnen grasslands and their responses to the East Asian Summer Monsoon (EASM)

Honghao Niu[a,1], Mengzhen Li[e,1], Laurent Marquer[f], Teija Alenius[g,1], Frank M Chambers[h], Dorothy Sack[i], Guizai Gao[a,b,c,d,*], Jiangyong Wang[a], Meng Meng[a], Linlin Liu[a], Lina Song[a], Anyi Xu[a], Dongmei Jie[a,b,c,d,*] jiedongmei@nenu.edu.cn

[a]School of Geographical Sciences, Northeast Normal University, Changchun, China

[b]Key Laboratory of Geographical Processes and Ecological Security in Changbai Mountains, Ministry of Education, Changchun, China

[c]Institute for Peat and Mire Research, State Environmental Protection Key Laboratory of Wetland Ecology and Vegetation Restoration, Northeast Normal University, Changchun, China

[d]Key Laboratory of Vegetation Ecology, Ministry of Education, Changchun, China

[e]College of Urban and Environmental Sciences, Peking University, Beijing, China

[f]Department of Botany, University of Innsbruck, Innsbruck, Austria

[g]Turku Institute for Advanced Studies, TIAS (Department of Archaeology), University of Turku, Turku, Finland

[h]Centre for Environmental Change and Quaternary Research, School of Natural and Social Sciences, University of Gloucestershire, UK

[i]Department of Geography, Ohio University, Athens, Ohio, USA

[*]Corresponding author at: School of Geographical Science, Northeast Normal University, Changchun, 130024, China.

Abstract

Exploring the Mid-Late Holocene interactions between ecological and climate variations in semi-arid areas such as Songnen grasslands (northeastern China) provide insights into how future vegetation changes and hydrological variations may have an impact on semi-arid ecosystems, in

[1] These authors contributed equally to this work

general. In this study, we present a high-resolution palaeoecological dataset covering the past 7300 years. For this purpose, a peat section has been sampled from the shore of Dabusu lake situated in the southwestern part of the Songnen grasslands. We use pollen analyses to reconstruct the regional and local vegetation dynamics, and measure TOC (total organic carbon) and the degree of peat humification to study changes in regional and local biomass. Diatom analysis, grain size analysis, and $CaCO_3$ contents are used to assess the water-table fluctuations of the Dabusu peatlands. The results show that from 7300-6000 cal BP, Dabusu peatlands were characterized by grasslands, dominated by Poaceae plants and high-water level. From 6000 to 910 cal BP, forest-steppes and dry-steppes dominated in the region alternatively. The water level of Dabusu peatlands experienced relatively low levels following an earlier rapid decline around 6000-5100 cal BP. Then after a slight increase between 5100 and 4000 cal BP, it remained at a relatively low level until 910 cal BP. After 910 cal BP, steppe vegetation dominated in the region and the water level of Dabusu peatlands slightly rose. By comparing these features with regional climate change, we show that EASM circulations might be the main driving forces controlling the regional paleovegetation dynamics and hydrological variations. This outcome is critical for the understanding of the long-term interactions between vegetation, hydrology, and climate of mid-latitude semi-arid grasslands.

Keywords

Holocene, Wetland, Monsoon, Grain-size, Pollen.

1. INTRODUCTION

Drylands cover approximately 41% of the land surface on earth and are home to more than 6.5 billion people worldwide (Reynolds et al., 2007). In China, drylands cover approximately 33% of the land surface and are characterized by diverse vegetation types ranging from true desert to scrub-woodlands with the semi-arid regions as the main dryland type in northern China (Zhu et al., 1980; Goudie, 2002; Yang et al., 2011). The ecosystem of drylands, especially in the mid-latitude semi-arid regions are sensitive to variations in temperature and precipitation, and have undergone severe land degradation and even desertification in recent decades. According to Huang et al. (2019), semi-arid areas have expanded nearly ten times faster over the last two decades than those in arid and sub-humid areas. This causes a severe threat to human activities, and in particular to

the present and future economic development of these regions (Dobie, 2001; Li, Gao & Han, 2017; Zhao & Yu, 2012; Li, Xie & Sack et al., 2021). In addition to drylands, lake systems in the semi-arid regions are also sensitive to climate change. Because of the ongoing global warming, the area of lake systems is constantly shrinking; lake basins and their surroundings are therefore more exposed to desertification (Ma et al., 2010; Tao et al., 2015; Chen et al., 2021). In order to set sustainable environmental policies and to implement ecological restoration projects, there is a need to assess the long-term impact of climate change on vegetation and hydrology dynamics (Khon et al., 2014; Liu, et al., 2005; Nelson et al., 2004; Zhao & Yu, 2012). The period since the mid-Holocene is particularly interesting as the global average temperature during the Holocene climate optimum was ca. 1-2 °C higher than the present (Gao et al., 2019). This can be seen as an analog for the ongoing climate warming as it has been predicted by the IPCC (Parchauri et al., 2014).

The responses of the ecological systems to climate changes are known to vary spatially and temporally (Brewer et al., 2017; Giesecke & Brewer, 2018; Huntley, 2010; Marquer et al., 2017; Zanon et al., 2018; Li et al., 2021). Hence, region-specific investigations of ecological dynamics induced by climate changes, and associated feedback mechanisms need to be conducted in semi-arid environments (Zhao et al., 2009; Zhao & Yu, 2012; Li, Xie & Sack et al., 2021). However, the understanding of long-term ecological dynamics in semi-arid regions is a challenging task owing to the difficulties in acquiring high-resolution sedimentary archives where biological proxies can be preserved (Goudie, 2002; Tooth, 2009). Most microfossils are not preserved in erosive and oxygen-rich conditions, such as sandy-paleosols and saline lakes, common in semi-arid regions. (Alexandre et al., 1997; Barboni et al., 1999; Boyd, 2005). This is particularly true for environmental proxies such as pollen that provide information about the past vegetation dynamics at century to millennial time scales (Horowitz, 1992; Li et al., 2017). Songnen grasslands, also known as Songnen sandy lands are located in the northeastern part of China and are transitional zones of Horqin sandy land and Greater Khingan Mountains' (Daxinganling) forests (Xiao, 1995) (Fig. 1a). Like semi-arid regions worldwide, paleoecological research in Songnen grasslands encounters the same problem in terms of finding suitable records, as the region has only sporadically distributed closed, shallow, alkaline lakes embedded in sandy

dunes (Li, 1991; Qiu et al., 1992). However, the high-resolution peat core present in this study provides the opportunity to get insights into the responses of the ecological systems to climate changes over a long-term perspective.

The regional climate of the Songnen grasslands is controlled by the low-latitude East Asian Summer Monsoon (EASM) and is influenced by mid-latitude westerlies (Zhang et al., 2003). Therefore, it is considered as an ideal pilot study region to assess the effect of past climate on vegetation and hydrology dynamics in semi-arid areas. The EASM circulations are mainly modulated by land-oceanic heat gradients that is controlled by changes in summer solar irradiation. When solar irradiation increases, the intensity of EASM is enhanced by the formation of a steep ocean/continent air pressure gradient; this mainly results from the heat capacity differences between the Asian continent and the Pacific Ocean accompanied by the northward movement of the Intertropical Convergence Zone (ITCZ) (Li et al., 2020). The strengthened EASM brings wet and warm maritime air masses moving into northeastern China and increases the precipitation of the study region. During periods of decreased solar irradiation, a relatively smaller differences in land-oceanic air pressure exists. A weaker EASM bring less moisture to northeastern China resulting in a decrease of precipitation in the study area (An, 2000; Wang et al., 2017).

Holocene vegetation and climate changes have been studied in Songnen grasslands from sandy-paleosol layers of sandy dunes using pollen information (Li, 1991; Li & Lu, 1996). However, pollen grains were poorly preserved in these sandy-paleosol sediments. Furthermore, the research was conducted with low temporal resolution and was focusing on the late Pleistocene rather than the mid-Holocene vegetation. The results of this study indicate that *Artemisia*-Chenopodiaceae grasslands dominated the region since the Mid-Holocene (Li, 1991; Li & Lu., 1996). Recent studies attempted to use phytoliths extracted from a sandy dune in central Songnen grasslands to reconstruct past vegetation; phytoliths are mainly composed of siliceous minerals and are therefore better preserved in such environmental contexts than pollen. By analyzing the assemblages of phytoliths, additional insights into the vegetation dynamics in Songnen grasslands have been obtained. In particular, the results show that since the start of the Holocene the region was characterized by Poaceae-dominant communities rather than

Artemisia-Chenopodiaceae communities (Li et al., 2017). However, one should consider the spatial representativeness of each proxy. Phytoliths are deposited in situ and would mainly reflect the local vegetation rather than the regional landscapes (Stromberg et al., 2018) when pollen would be representative of a mix of local and regional vegetation. A high-resolution pollen record is needed to contribute to this debate about the vegetation dynamics since the mid-Holocene in the Songnen grasslands.

Hydrological research focusing on the mid-Holocene are hardly find in this region. This is mainly explained by the fact that the lake sediments of the region covering this time period do not have high temporal resolution to conduct reliable sampling for multiproxy analyses (Li et al., 2019). Undeniably, hydrological research are necessary to understand the climate changes since the mid-Holocene in the Songnen grasslands.

Besides climate oscillations, it has been suggested that EASM played a significant role to explain the long-term vegetation dynamics and hydrological variations in Songnen grasslands (Li & Lv, 2001; Zhang et al., 2017). It is known that the EASM associated precipitation patterns largely control the vegetation distributions of the Songnen grasslands, except for the vegetation largely influenced by human activities.

In order to test this hypothesis, we present here a high-resolution and well-dated multi-proxy records from the Dabusu peatlands. These peatlands are formed on the lakeshore of the Dabusu lake, which is located in the southern Songnen grasslands. The water might have covered the peatlands during the humid climate period when the Dabusu lake had a high water-table condition. However, in the past few decades, the Dabusu lake was in a low water-table condition and the water table had retreated far away from the current peatlands. Note that although changes in the water-levels of the peatlands are closely related to the water-table of the lake, the variations of the lake levels are not the only drivers of change in the water levels in the peatlands, other factors such as seasonal snow-melt can also contribute to the temporary high water level of the peatlands. The whole 300 cm peat core covering the past 7340 years has been collected and analyzed for pollen, diatom, grain-size, total organic carbon (TOC), organic carbon content ($CaCO_3$), and

degree of peat humification. The aims of the present study are to:

1) reconstruct the past vegetation dynamics of the Songnen grasslands

2) assess the water level changes of the Dabusu peatlands

3) discuss the responses of past vegetation and hydrological variations to climate changes by comparing our results with the existing Holocene climate records.

2. REGIONAL SETTING

The Songnen grasslands (44º45′-48º20′N, 120º40′-126º00′E) are located at the eastern margin of the Eurasian steppe belt in Northeast China. The semi-arid climate of the region is influenced by the East Asian monsoon system and is characterized by short summers and by warm and humid air transported from the Pacific Ocean and Indian Ocean. The dominant northwesterly winds bring cool and dry air in long winters. The average annual temperature today increases from 3.5 ºC to 5.0 ºC from north to south, while the average annual precipitation varies between 320 mm to 480 mm from west to east, respectively (Li, 1994). The total annual precipitation is 360 mm, of which at least 70% is received during the growing season. The evaporation rate is high, about 1600mm/year (Xiao, 1995).

The topography of the region is characterized by sandy dunes and interdune lowlands, with an elevation range from 130 to 160 m. The semi-arid climate supports short and scrubby dry steppe vegetation, dominated by Poaceae taxa such as *Leymus chinensis*, *Stipa baicalensis*, *Arundinella hirta*, growing mainly on the interdune lowlands while shrubs and xerophytic plants such as *Artemisia*, Chenopodiaceae, and Asteraceae are widely distributed on the sandy dunes.

Lake Dabusu (44º49′48.4″N, 123°40′27.2″E; 27m) is located on the Qian'an highland in the southern part of Songnen grasslands, in the province of Jilin in north-eastern China (Fig. 1). The lake is about 37 km^2 in size, with 0.5-1.5 m water depth depending on the various seasonal precipitation and underground water replenishment. The lake is an alkaline lake with a pH value ranging between 9.55 and 10.55. Peatlands dominate the northern lakeshore and the local vegetation is mainly characterized by sedges and other helophytes. Over recent decades, the

vicinity of the lake has been transformed into agricultural land, mainly growing crops including rice and corn.

3. MATERIALS AND METHODS

3.1. Sample collection and chronology

The peat was cored in the summer of 2016, using a piston corer, from the northern side of the lake (Fig. 1B). In total, a 300 cm long peat profile has been retrieved. The Dabusu peat (LDBS) core was cut into 6 sections in the field and then wrapped in polyvinyl chloride (PVC) tubes for transfer. In the laboratory at Northeast Normal University, the peat sections were split open and sampled at 1 cm resolution for pollen, diatom, grain size, TOC, $CaCO_3$, and peat humification analyses. The peat profile was dated by means of seven accelerator mass spectrometry (AMS) dates obtained from bulk organic samples and plant residues at Guanzhou Institute of Geochemistry, Chinese Academy of Science (GIGCAS) (Tab. 1). All ages were calibrated into calendar years with the IntCal20 calibration curve (Reimer et al., 2020) using the CALIB 8.10 program (Stuiver and Reimer, 1993). “Rbacon” package (v 2.5.0) was used to create the chronology (Fig. 2).

3.2. Laboratory work

In total 300 peat samples, obtained at 1 cm resolution from the Dabusu peat profile, were taken for pollen. Sub-samples for pollen analysis were prepared according to the standard alkaline and acidic processing method described in Faegri and Iversen (1989). To remove clay-sized particles, the samples were sieved using a 10 μm screen. For calculations of pollen concentrations (number of pollen grains per cm^3 of sample), one *Lycopodium* tablet (Stockmarr 1971) was added to dry samples of 5 g (18,583 grains per tablet). This was followed by treatments with HCL, NaOH, HF, and a hot acetylation mixture. At least 300 pollen grains including both terrestrial and aquatic pollen types were counted for each sample under × 400 magnification. The identification of pollen species was based on the publications of Wang et al. (1995) and Xi & Ning (1994). Pollen percentages were calculated on the basis of sum of terrestrial pollen grains. The percentages of aquatic pollen/spores were calculated based on the sum of terrestrial pollen and aquatic pollen/spores.

The diatoms were analysed at 2 cm intervals from the peat sequence. The samples were pretreated as follows: 10% hydrochloric acid (HCl) was used to remove carbonates before washing the samples with distilled water, then 30% hydrogen peroxide (H_2O_2) was added to remove organic matter, followed by another washing step using distilled water. Density separation to extract diatoms has been performed by using $ZnBr_2$ (density of 2.30 g/cm^3). Each sample was washed and rinsed by distilled water and ethanol before applying Canada balsam with a refractive index of 1.5216–1.5240. Identification follows Hargan et al. (2015) and Chen et al. (2016). A minimum of 300 frustules was counted per sample. For diatom data analyses, a relative abundance of each diatom taxa was calculated.

The grain size analysis was determined at 1-cm resolution. The pretreatment process follows Hao et al. (2012). The samples (of approximately 1 g) were sieved using a 2 mm mesh and first pretreated by 30% hydrogen peroxide (H_2O_2) for 3 hours and then 10% hydrochloric acid (HCl) for 2 hours at 100 ℃ in a water bath to remove organic matter and carbonates. The samples were then dispersed by adding 10 ml 0.05 mol/L $(NaPO_3)_6$ and shaken on an ultrasonic device for 20 min. Grain-size frequency distributions were measured using a Microtrac S3500 particle analyzer. Statistical parameters of samples such as fractions, median diameter (Md) (μm), standard deviation, skewness, and kurtosis were assessed.

The total organic carbon (TOC) and carbonate contents ($CaCO_3$) was determined at 2 cm intervals according to the procedures described by Li (2020). For the determinations, 1g dry samples (oven-dried in 105 °C) were first placed into quartz boats. The organic matter and carbonate contents were combusted under O_2, using a muffle furnace at a temperature of 550 °C and 900 °C, respectively. TOC content and organic carbon content of each sample were calculated according to Eq. (1) and Eq. (2), respectively.

$$\mathrm{TOC_{LOI}}\% = \frac{0.58\times(m_{105}-m_{500})}{m_{105}} \times 100\% \qquad (1)$$

$$CaCO_{3_{LOI}}\% = \frac{(m_{500}-m_{800})}{0.44\times m_{105}} \times 100\% \qquad (2)$$

Here, m105 is the sample weight dried at 105 ℃, and m500 and m800 are the sample weights after combustion at 500 ℃ and 800 ℃. The value 0.58 is the soil organic matter (SOM) to soil organic carbon (SOC) conversion factor (Pribyl, 2010) and 0.44 is a conversion factor to transfer 800 ℃ weight loss to $CaCO_3$ content (Yang et al., 2016).

The degree of humification was determined at 2 cm intervals using the alkali-extraction method (Chambers et al., 2011). The dry samples of 2 g in size were ground and sieved by a 60-mesh screen before mixing. 50 ml 8% NaOH solution was then added to each sample and heated at 100 ℃ for 1.5 hours in order to extract humic acid. After cooling, 20 ml top layer solution was moved into another 100 ml flask by adding 80 ml distilled water. A Spectrum722 spectrometer was used to test the absorbance value compared to distilled water as the blank with a wavelength of 540 nm. The obtained absorbance value is used to express the degree of peat humification.

3.3. Numerical methods

The pollen and diatom diagrams were plotted using the TILIA software (v 2.0.41) (Grimm, 1991). Stratigraphically constrained cluster analysis program CONISS was performed in order to identify periods of similar vegetation composition based on the pollen data, and the CONISS was also used for diatom to establish their biostratigraphic zones (CONISS; Grimm 1987).

For diatoms, principal component analysis (PCA) was performed to assess the main environmental factors that can explain the temporal variations in diatom assemblages. PCA was conducted by using the *procom ()* function in R with the default "stats" R package, and graphs of eigenvalues and diatom types were performed by using the R package “factoextra” (Kassambara & Mundt, 2019).

End-member modeling analysis was performed for the grain-size dataset using the ‘AnalySize modeling algorithm’ in Matlab (v 7.6) program (Paterson and Heslop 2015). The program

transforms the grain-size frequency distributions into several unimodal grain-size end members (EMs). Note that the end members are interpret individually.

4. RESULTS

4.1. Chronology

Age determinations are expressed in cal. yr BP with 2σ ranges and median ages (Table 1; Fig. 2). The age-depth model is based on six AMS dates obtained from the peat sequence (Fig. 2), and shows a continuous deposition of peat sediments from at least about 7180 cal BP (290 cm; NENUR 10486) to 190 cal BP (35 cm; NENUR 10479). The average deposition rate is 0.44 mm per year. In Table 1, LDBS 4 and LDBS 6 show chronological inversions. This is certainly related to the coring of the lake shore that may be influenced by the water level fluctuations. During the low lake levels, hiatuses might exist when no hiatuses would be present during the high lake levels.

4.2. Pollen

In general, herb pollen dominates in the pollen spectra. The mean pollen percentage from herbs over the last 7300 cal BP is 78.8%. The most common herb pollen types are *Artemisia* (mean 20.5%), Chenopodiaceae (mean 14.5%), Poaceae (mean 8.7%), Cyperaceae (mean 28.6%), and Asteraceae (mean 4.1%). The mean of pollen percentages from trees over the last 7300 cal BP is 17.6%. The major tree pollen types are *Pinus* (mean 13.3%), *Quercus* (mean 3.8%), and *Ulmus* (mean 1%). *Typha* and ferns are also recorded with means pollen percentages over the last 7300 cal BP of 10.8 % and 4.9%, respectively. Pollen concentration ranges from 0.9×10^3 to 234.7×10^3 grains/g with a mean value over the last 7300 cal BP of 24.4×10^3 grains/g. According to the CONISS analysis, the pollen diagram is divided into four pollen assemblage zones (Fig. 3). Zone 1 is subdivided into two subzones, 1a and 1b.

Zone 1 (300-215 cm) : 7300-5100 cal BP

The subzone 1a (300-250 cm, 7300-6000 cal BP) is characterized by high percentages of *Typha* (with a mean of 42.4% for the subzone) and lower percentages of herb pollen types compared to

the later periods. The most abundant herb taxa are *Artemisia* (8.8-41.9%), Chenopodiaceae (5.2-24.8%), Cyperaceae (0.2-53.1%), and Poaceae (2.7-22.5%). Tree pollen is present in low proportions (with an average percentage of 14.7%), and deciduous broad-leaved trees *Quercus* and *Ulmus* are present in ca. 7.0% and 1.3%, respectively. Pollen concentration shows an increasing trend (from 2.3 up to 234.7 $\times 10^3$ grains/g) throughout the subzone.

The subzone 1b (250-215 cm, 6000-5100 cal BP) is dominated by a gradual decrease in *Typha* percentages (from about 57.2% to 8.3%) accompanied by an increase in tree and herb taxa pollen. Herb pollen types have a mean percentage within the subzone of 80.1%. Tree pollen types increase from 6.7 to 47.8%, with a notable increase in *Pinus.* Between 6000 and 5800 cal BP, pollen concentration peaks, reaching a value of about 90×10^3 grains/g, and then decreases to about 30×10^3 grains/g.

Zone 2 (215-170 cm): 5100-3800 cal BP

This zone is also dominated by herb pollen (mean 76.9%). Asteraceae and Cyperaceae pollen are increasing; they have a mean percentage over the zone of 11.3% and 29.2%, respectively. *Pinus* percentages increase further compared to the previous zone with a mean value of 15.0%, while *Quercus* percentages fall slightly. *Betula* is continuously present over zones 1 and 2, and *Typha* percentages are further reduced. Both the percentage of *Abies/Piceae* and *Tsuga* reached their peak values of 10.1% and 10.2% at 5000 cal BP and 3900 cal BP, respectively. The pollen concentration is similar to that in subzone 1b.

Zone 3 (170-60 cm): 3800-910 cal BP

The percentages of herb pollen types decrease slightly at the start of pollen zone 3 and then increase again, with a mean of 73.5%. The tree pollen mean is 25.8% in, which is an increase compared to zone 2. High percentages are recorded for *Artemisia* (mean 20.1%), whereas the Chenopodiaceae (mean 13.6%) and Poaceae (mean 8.8%) percentages remain stable. Pollen from Cyperaceae fluctuate between 6.1% and 59.5% over zone 3. *Pinus* percentages are high (mean 20.5%) particularly in the first half of the zone until ca. 2500 cal BP. *Quercus* pollen do not show specific differences compared to zone 2, although the percentages are slightly higher after 2500 cal BP. *Ulmus* percentages increase until ca. 2500 cal BP and then decrease.

Zone 4 (60-0 cm): 910 cal BP - present

The uppermost zone is characterized by an increase in herb pollen percentages with a peak (96.6%) at 564 cal BP. In addition, the percentages of fern spores rise to reach the highest values over the last 7300 cal BP. Within herb pollen types, the highest percentage increases correspond to Cyperaceae, with a zone 4 mean of 34.0%. Pollen from *Artemisia* (mean 19.6%) and Poaceae (mean 7.8%) decrease slightly compared to zone 3. *Pinus* (mean 10.7%) and *Quercus* (mean 2.2%) are present in lower percentages than in zone 3.

4.3. Diatoms

4.3.1. Past dynamic of diatom assemblages

Twenty-three diatom species were identified in the Dabusu peat sequence (Fig. 4.). The diatom stratigraphy was divided into four CONISS zones. Considering th core as a whole, the *Epithemia adnata* species dominated the diatom assemblages, having a mean abundance of 47%.

Zone I (300-241 cm) : 7300-5800 cal BP

During this period, the abundance of *E. adnata* fluctuated sharply between 15% and 52%. *E. turgida*、*A. granulata*、*C. aspera*、*Amphora copulata*、and *Gomphonema spp.* all reach their maximum percentages while the proportions of *E. adnata* decreases over this interval.

Zone II (249-72 cm): 6000-1200 cal BP

The period 6000-910 cal BP is mainly characterized by *E. adnata* taxa. The percentage of both *H. amphiaxys* and *Diplonies spp.* reach their maximum values in 4000 cal BP and 2800 cal BP, respectively.

Zone III (72-0 cm): 1200 cal BP-present

After 1200 cal BP, the abundance of *E. adnata* decreases gradually remaining at its lowest level for the core at a mean percentage of 34.9%. The abundance of *Rh. musculus* increases rapidly and becemes the dominant taxon. The percentags of *Pinnularia spp.* also increases during the period.

The three main PCA components explain together 56% of the total variance in the diatom assemblages. Component 1 (PCA1) explains 27.9% of the variations while component 2 (PCA2) explains 15.7%. Fig. 4 shows that PCA1 scores increase rapidly then remain at a high level in Zone I with a mean value of 1.17. PCA1 scores decline abruptly and fluctuate at a relatively low level in Zone II. Finally, PCA1 scores increase slightly and reach a relatively high value in Zone III.

4.4. Grain-size analyses

The Dabusu peat samples have a grain-size range from 2 to 300 μm. Mean grain size (Md) of individual samples range from 23 to 132 μm, and the average Md of all samples (n=300) is 42 μm. Silt and sand dominate the sediments. In addition, both bimodal and unimodal grain-size distributions are observed. The end-member analysis reveals unbiased subpopulations of grain-size distributions to display sedimentological information (Weltje & Prins, 2007). Goodness-of-fit analysis shows a better fit (higher R^2) when using more end members (EMs) (Fig. 6). However, a comparatively modest number of EMs is advocated for meaningful interpretation of compositional variation. The two criteria used for selecting the approporiate number of end members are parsimony and reproducibility (Jiang et al., 2020). The ideal is to choose the minimum number of end members (parsimony) that explain over 95% of the variance of the entire grain-size dataset. Therefore, a three-EM model was selected that explains 97.9% of the variance of the entire data set. The modeled median values of these EMs are 17.38 μm (EM1), 53.36 μm (EM2), and 98.05 μm (EM3) (Fig. 7).

The relative abundance of EM1 varies significantly between 0 and 90.7%. The EM1 values increase sharply from 4.4 % to about 59.1% between 7300 and 6000 cal BP (corresponding to 300-250 cm of the section), then slowly increases to about 70.7 % at 5100 cal BP. The values then fluctuate from 32.2 % to 90.7 % between 5100 and 900 cal BP, followed by a declining trend in the uppermost 50 cm (since 910 cal BP). The variation trend of EM2 values remain relatively stable (around 35.7%) during the sequence. High EM3 values are recorded in the lowermost part of the record (during 7300-6000 cal BP), but the values quickly decrease and remain in a relatively low range for the rest of the sequence. Moreover, the variation trend of mean grain-size

values shows a similar pattern with EM3 values (Fig. 8).

4.5. General changes in TOC, $CaCO_3$, and Peat humification degree

Carbonates are the main salts in the sediments of the Dabusu peatlands, and they show some trends similar to the PCA1 scores of the diatoms (Fig. 8). Between 7300 and 6000 cal BP, the $CaCO_3$ content is high, reaching maximum values (27.7 %) at 6400 cal BP. $CaCO_3$ content then decreasse between 6000 and 4700 cal BP. After 4700 cal BP, $CaCO_3$ content increases, followed by a a slight decreasing trend, and then rises over the last centuries to a relatively high value. Changes in TOC and degree os peat humification degree similar trends with the core. They both increase from 7300 to 5100 cal BP, decrease until ca. 2500 cal BP, then rise again. After 910 cal BP, the values flucuate.

5. DISCUSSION

5.1. Pollen taphonomy

In the semi-arid region of the Songnen grasslands, *Artemisia* and Chenopodiaceae dominate the present and past pollen assemblages. In order to assess changes in aridity of the study region, we have calculated the ratio between *Artemisia* and Chenopodiaceae (A/C) pollen types. Previous research in the Tibetan plateau and grasslands of northern China have reported that A/C values are often below 0.5 in the desert and desert steppe, ranging from 0.5-1.5 in the dry steppe, fluctuating between 1.5-5 in the steppe, and reaching above 5 in the meadow (Yan, 1991; Yu et al., 1998; Li et al., 2005a; Zhao & Herzschuh, 2009; Li et al., 2010). The A/C ratio, however, should be used carefully because it can be influenced by elevation, human activity, and other non-climatic factors (El-Moslimany, 1990; Cour et al., 1999; Liu et al., 2006). In the present study, the A/C ratio might be a reliable indicator to distinguish different vegetation types, this for the following reasons. First, Songnen grasslands are considered as a semi-arid region in northeastern China, and A/C ratios have been considered as a reliable indicator in most semi-arid and arid regions worldwide (Li et al., 2010). Moreover, studies have been using the A/C ratios to differentiate steppe, desert steppe, and meadow in Innermogolia grasslands- the adjacent region of the Songnen grasslands (Li et al.,

2005a; Li et al., 2005b). Considering the similarities of the vegetation structure and composition of the Songnen grasslands and Innermogolia grasslands, one can assume reliable the A/C ratio in our study area. Note that the A/C ratios might not be a reliable indicator in intensive human-induced vegetation contexts, however, human activities were rare over the past thousands of years in Songnen grasslands (Zhao, 2014; Jia et al., 2016).

The pollen data from the Dabusu peat sequence show that *Artemisia*, Chenopodiaceae, Cyperaceae, and Poaceae are the most abundant herb pollen types, while the most abundant arboreal pollen are *Pinus* and *Quercus*. Among the dominant herb pollen types, Cyperaceae pollen represents the local vegetation growing on the peatlands, whereas *Artemisia*, Chenopodiaceae, and Poaceae, because of relatively high pollen productivity and dispersal properties, likely represent the more regional background pollen and, therefore, the regional vegetation (Xu et al., 2007; Li et al., 2010; Sjogren et al., 2015; Li, 2020). *Artemisia* and Chenopodiaceae are high pollen producers, and the pollen taxa of these species are over-represented in the pollen assemblage compared to the actual vegetation (Zhao et al., 2008; Sjogren et al., 2015); this fact is now commonly accepted by the pollen research community. For example, in the study of Li et al. (2015), *Artemisia* and Chenopodiaceae pollen types dominate the pollen assemblages resulting from surface soil samples collected in steppes dominated by Poaceae plants; Poaceae pollen percentages of these samples are only around 7.5%. Studies by Li et al. (2013, 2015) further demonstrated that *Artemisia* and Chenopodiaceae pollen percentages can each reach approximately 20% of the pollen assemblages of grasslands and their percentages can be large a in forest landscapes that are characterized by few *Artemisia* and Chenopodiaceae plants. Preservation in soil samples can be a factor in the over-estimations of *Artemisa* and Chenopodiaceae pollen types which are known to be more resistant than other pollen types, such as Poaceae and tree pollen, to taphonomical processes affecting the soil samples.

Regarding the arboreal pollen types, *Pinus* pollen percentages alone cannot be considered as a reliable indicator to assess grassland versus forest landscapes at a local scale. *Pinus* pollen are spread over long distances and *Pinus* plants are high pollen producers. This helps explain why *Pinus* pollen are regularly found in topsoil collected in steppe and desert environments where it

can exceed 30% of the total pollen assemblages (Xu et al., 2007a). Furthermore, *Pinus* pollen percentages can reach 10% in samples collected from steppe and desert regions when *Pinus* trees are absent in the present vegetation (Li & Yao, 1990; Xu et al., 2007b). Similar to the *Pinus* pollen, *Betula* pollen percentages can also over-represent their vegetation cover owing to their long-distance transportation ability (Xu et al., 2007a). On the other hand, past research has shown that *Quercus* pollen percentages exceed 10% in *Quercus* forests and are lower than 1% where few *Quercus* trees exist, thus the 3.8% mean *Quercus* pollen percentage in this study indicates that *Quercus* trees were distributed sporadically in the Songnen grasslands (Xu et al., 2007a; Li et al., 2015). In our study, *Ulmus* pollen is recorded in low abundances throughout the peat core. Previous studies have shown that *Ulmus* pollen percentages in topsoil are about 10% in *Ulmus*-dominated forests, and constitute less than 1% where *Ulmus* trees do not dominate the forests (Li et al., 2005; Xu et al., 2007b). Considering the low percentage of *Ulmus* pollen in topsoil samples collected in a landscape dominated by *Ulmus* plants, *Ulmus* trees were probably growing near the Dabusu peatlands since the Mid-Holocene. *Carpinus* pollen also stays at a relatively low level through the whole peat section, but its pollen percentage can accurately represent its vegetation cover (Xu et al., 2007a). Regarding the aquatic pollen types such as *Typha*, their abundances are certainly related to the water level changes, in particular they would refer to shallow water conditions (Huang et al., 2010; Xiao et al., 2021). Finally, fern spores are found in relatively low percentages in forest topsoil samples compared to surface soil samples in grasslands, and fern percentages in the Dabusu peat maintained relatively high amounts with a mean percentage of 4.9% in the present study (Li et al., 2015).

5.2. Sedimentary processes

The end-member approach for grain-size analysis of the Dabusu peatland sediments suggests a unimodal grain-size distribution for the three types of particles. EM1 represents the finest particle fraction with a mean grain size of 18.33 μm. Typically, fine particles smaller than 20 μm can travel up to thousands of kilometers (Pye, 1987; Shao, 2008; Stuut et al., 2009). Previous studies have shown that sandstorms with the mean grain size ranging from 10 to 20 μm frequently take place in northeastern China during the spring. The frequency of sandstorms is controlled by the strength of the East Asia Winter Monsoon (EAWM) which can transport fine particles from the Loess Plateau

and desert of northwestern China directly to northeastern China. Hence, we consider that EM1 represents aeolian dust transported during sandstorms.

The mean grain modal size of EM2 is approximately 55.61 μm. Particles of this size are transported fewer than several hundreds of kilometers (Shao, 2008). Particles of the top layer of sand dunes from the Horqin sandy land, situated about 50 km from the Lake Dabusu (adjacent to the western margin of the Songnen grasslands) are found to be about 50 μm. This is consistent with the mean particle size of EM2 (Cao et al., 2005; Shen et al, 2016; Zhang et al., 2020). We therefore argue that the source area of EM2 grains is the Horqin sandy land.

With a mean grain size of 99.50 μm, EM3 represents the coarsest component of the peat samples. In summer, increased seasonal precipitation and the resulting runoff from the slopes causes an increase in coarse particles being transported from higher elevation surrounding areas to the peatlands (Li et al., 2014; Zhang et al., 2014). The corresponding transportation mode of these particles should be saltation influenced by the hydrodynamic force (Shao, 2008). Therefore, we argue that the fluctuation of EM3 values represents hydrological variations of the Dabusu peatlands. The hydrological significance of the coarser fractions in peatlands is currently still unclear (Mancini, 2009; Vis et al., 2010).

The modern samples' grain size distributions in peatlands (covered by water all year round) have shown that Md increases while the water level decreases. This is because coarser materials are more liable to be deposited in marginal areas with a lower water table (Zhang et al., 2021). As the water level rises and covers the peatlands, fewer coarse fractions are carried to the center of the peatlands owing to the larger distance from the center to the shoreline (Chen et al., 2021).

Furthermore, studies of surface sediments conducted in the center of the lake and lakeshores show that Md positively correlates with the water level of the peatlands, possibly because the peatlands are formed on the lakeshores and are not covered by water most of the time (Xiao et al., 2013). Therefore, it can be assumed that the increase of seasonal precipitation resulted in the rise of the

water level of the peatlands. At the same time, coarser materials would have been carried out to the peatlands. All of this would explain the increase of Md.

Because the deposition of carbonates is a complex process related to interactions among geology, climate, sedimentary types, and hydrochemical conditions, the relationships between salt, $CaCO_3$ content, and water level is region-specific (Hofmann, 2005; Francke et al., 2013). Jie et al. (2001) showed that $CaCO_3$ content varies in lake surface sediments from the lake center to the lakeshore. In addition, their results show a positive relationship among salt, $CaCO_3$ content, and lake level, which can be a reference for water-table reconstruction of the Dabusu peatlands in this study. In the following sections, the hydrological variations in Dabusu peatlands are discussed in detail.

5.3. Environmental influences on diatom assemblages

In the entire sedimentary section, except for the planktonic species *Aulacoseira granulata*, all observed species favor benthic habitats that commonly occur in saline freshwater contexts; this would refer to little habitat changes (Serieysssola, 2012; Hargan et al., 2015; Chen et al., 2016). As a result, the plankton/benthos (P/B)-ratio in the present study cannot be used to interpret changes in water level at the Dabusu peatlands. Instead, PCA is used to identify the dominant factors associated with variations of diatom assemblages to investigate water-level fluctuations.

According to the PCA plot (Fig. 5), diatoms including *Gomphonema spp.*, *Amphora copulata*, *E. turgida*, and *Aulacoseira. granulata*, which have tolerant of salt habitats, have the highest positive distributions along PCA 1. Conversely, *E. adnata* and *Hantzschia amphioxys*, diatoms that favor freshwater environments (Denys, 1991; Dam et al., 1994), have negative distributions along PCA 1, suggesting that PCA1 represents salt content of the Dabusu peatland sediments. Therefore, positive distributions along PCA 1 likely indicate higher salt contents, whereas negative ones represent lower salt contents. Diatom species, such as *Rhopalodia musculus*, *E. adnata*, *Diplonies spp*, and *Cymbella aspera*, which prefer living in a relatively warm water body (Stockner, 1967), have positive distributions along PCA2. *E. adnata* and *C. aspera*, which favor low-temperature environments (Owen et al., 2008), have negative distributions along PCA2. Temperature variations of the peatlands appear to regulate diatom distribution along PCA2. In the Dabusu

peatlands, salt content varies with water-table fluctuations. Therefore, only PCA1 scores are used for water-table reconstructions and related analyses in the following sections.

5.4. Holocene environmental changes of Songnen grasslands

5.4.1. Holocene vegetation dynamic

The pollen record from the Dabusu peat sequence indicates that steppe was the most abundant vegetation type in the region after the Mid-Holocene with forest-steppe, that is, a steppe-like environment with sparse woody taxa, developing from 3800 to 910 cal BP. The local landscape was mainly characterized by meadow type vegetation with a high abundance of Cyperaceae plant taxa, which prefer moist environments typical of peatlands. Meanwhile, changes in TOC and degree of peat humification relate directly to variations in biological productivity and can indirectly reflect changes in the relative vegetation cover and vegetation diversity (Zuo et al., 2011; Zhang et al., 2012).

More specifically, from 7300 to 6000 cal BP (Zone 1a), the A/C ratios were mostly above 1.5 (Fig. 9) indicating that the regional steppes were represented by an abundance of *Artemisia* (mean pollen percentage of 14.5%), Chenopodiaceae (mean pollen percentage of approximately 8%), and Poaceae. Broadleaf trees, such as *Quercus* and *Ulmus*, were growing in the vicinity of the peatlands while *Birch and Carpinus* trees also show relatively high abundance at those times. In addition, *Typha* was abundant locally on the lakeshores. The local landscape was likely wet meadows characterized by Cyperaceae. The abrupt increase in TOC values and degree of peat humification indicate high biological productivity around the Dabusu peatlands, reflecting a relatively high vegetation cover and biodiversity of the region (Fig. 9).

From 6000 to 5100 cal BP (Zone 1b), the A/C ratio fluctuates around 1.5 (Fig. 9), which points to a dominance of steppes and dry steppes in the region. The abundance of local *Typha* plants decreases while abundances of *Pinus* trees gradually increase in the region. The decrease in TOC indicates a decline in biological productivity, while the peat decomposition rate remains high (Fig. 9). Despite vegetation cover and biodiversity starting to decrease, a high rate of decomposition

was maintained in the peatland because of the large amount of plant residue that had accumulated in the previous period.

Between 5100 and 3800 cal BP (Zone 2), a dry steppe dominated by *Artemisia*, Asteraceae, and Chenopodiaceae plants occupied the regional landscape; the A/C ratio from this zone is generally less than 1.5 (Fig. 9). *Typha* abundance decreased in the local vegetation while Cyperaceae dominated the local moist meadows. The regional abundance of *Pinus* expanded further. Broadleaved trees decreased slightly both locally and in the region. That biological productivity continued to decrease reaching its minimum in this interval follows from vegetation cover and biodiversity falling to their lowest levels, as reflected in the low values of both TOC and degree of peat humification (Fig. 9).

From 3800-910 cal BP (Zone 3), the A/C ratio was generally above 1.5 and the percentage of arboreal pollen increased abruptly (Figs. 3 & 9). These data indicate that the regional landscape was characterized by forest-steppes with the forest and steppe plant communities essentially corresponding to coniferous trees (particularly *Pinus*) and Poaceae plant taxa, respectively. The local vegetation was similar to what it was during the previous periods. Moreover, both TOC and degree of peat humification increased, indicating that biological productivity rose and therefore that vegetation cover and biodiversity might have already gradually recovered (Fig. 9).

After 910 cal BP (Zone 4), the regional landscapes gradually transformed from forest-steppe to dry steppe then to steppe. The A/C ratios show an increasing trend over the last 5 centuries when the abundance of Cyperaceae rose at the local scale (Fig. 9). Meanwhile, the increasing trend in TOC and peat accumulation rates indicate a slight increase in biological productivity related to the slight increase of the vegetation cover and biodiversity.

5.4.2. Holocene hydrological variations

The continuous decrease in both EM3 and mean grain size from 7300-6000 cal BP indicate that precipitation gradually diminished over this interval (Fig. 9). The high abundance of *Typha* pollen, characteristic of aquatic environments, and the maximum value of PCA1 scores and salt/$CaCO_3$

content, however, indicate that the water level remained high at the Dabusu peatlands.

The gradually decreasing *Typha* pollen percentages between 6000 and 5100 cal BP represent a lowering of the water level. At the same time, EM3, mean grain size values, PCA1 scores, and $CaCO_3$ content remain relatively low, suggesting that although the the water-level is low, the environment is still damp. During 5100 cal BP to 4000 cal BP, *Typha* pollen percentages remain at low values, while the $CaCO_3$ content increased to relatively high levels, possibly because the lake level increased and low water conditions existed at the sampling site. Low values of the same four variables point to a low water level and long-term arid conditions from 4000 cal BP until 910 cal BP. A sudden increase of $CaCO_3$ content and mean grain size and the sudden appearance of *Typha* pollen around 4000 cal BP might reflect a temporary rise in water level, possibly caused by a series of extreme rainfall events. A slight increase in mean grain size after 910 cal BP indicates a water-level rise. PCA1 scores and $CaCO_3$ content also show a sharp increase at the end of that period.

5.5. Influence of Holocene climate changes on the environmental context of the Songnen grasslands

Comparison of the vegetation dynamics and water-level reconstructions of the Dabusu peatlands with regional climate variations is shown in Fig. 9. The trends in EASM variations have been generally consistent since the Mid-Holocene in marginal EASM regions, with decreasing moisture levels due to continuously weaker summer solar insolation (Berger et al., 2007; Chen et al., 2008).

A relatively high EASM index and low stalagmite $\delta^{18}O$ value from Nuanhe cave suggests that intense EASM stages occurred between 7300 and 6000 cal BP (Wu et al., 2011). The strong EASM brought more moisture and precipitation to the study area, causing the water level to rise in the low-lying Dabusu peatlands. The humid climate provided favorable conditions for the Poaceae-dominated steppe to expand in the Songnen grasslands. The EASM weakened abruptly between 6000 and 5100 cal BP, with a notable decrease in precipitation and moisture (Xu et al., 2019; Zhang et al., 2021; Zhang et al., 2011). This, in turn, led to lowering of the water level at the Dabusu peatlands; regionally, the vegetation oscillated between steppe and dry-steppe.

The period between 5100 and 910 cal BP was characterized by a weak EASM, low precipitation, and a relatively arid climate that led to a low water level at the peatlands, although EASM intensified during the period between 5100 cal BP and 4000 cal BP (Huang et al., 2021). Dry-steppe dominated the region while forest-steppe occurred sporadically. After 910 cal BP, the EASM strengthened slightly, which is consistent with the increase in regional mean annual precipitation (MAP) and moisture and a slight rise of the Dabusu peatland water level. Steppe, controlled by climate change, became the dominant regional vegetation type.

In addition to the EASM, oscillations in other climate variables influence regional vegetation dynamics and hydrological variations in this study area. The reconstructed water levels of the Dabusu peatlands closely agree iin timing with the stacked ice-rafted debris (IRD) events identified in the North Atlantic Ocean (Bond et al., 2001). High-latitude land areas bordering the North Atlantic and North Pacific Oceans were notably influenced by these global climate cooling events in which a decrease in solar irradiance led to increased polar ice volume that directly reduced North Atlantic deep water (NADW) circulation. Regional vegetation dynamics are also sensitive to the IRD events, indicated by the expansion of the *Pinus* forests during IRD2 and IRD1.

Since the mid-Holocene, dominant local vegetation in the vicinity of the Dabusu peatlands varied between aquatic plants or hygrocolous plants in response to water-level fluctuations. During periods in which high water levels covered the peatlands, aquatic plants, especially *Typha*, were abundant. Even when the water level was lower, local environmental conditions remained humid because of thelow relief in the peatlands. These humid conditions, in turn, led to the widespread growth of sedge-dominated meadows. Therefore, local hydrological conditions, rather than regional climate change, are considered the main driving force for local vegetation change.

In summary, the EASM and associated precipitation variations caused by solar irradiation anomalies directly controlled water-level fluctuations of the Dabusu peatlands. These local hydrological variations subsequently drove the local vegetation evolution of the study area.

Regional vegetation dynamics were mainly controlled by EASM variations but were also influenced by IRD events.

6. CONCLUSIONS

This study presents a high-temporal resolution of pollen ,diatom and sedimentary records from the Dabusu peatlands covering the Mid-Late Holocene. It provides new insights into the vegetation dynamics and hydrological variations in Songnen grasslands and their responses to the EASM.

In particular, steppe vegetation, dominated by Poaceae, characterized the Songnen grasslands from 7300 until 6000 cal BP. This was followed by a period of dry steppe vegetation from 6000 cal BP until 3800 cal BP. From 3800 until 910 cal BP, the region varied between forest-steppe and dry steppe. After 910 cal BP, the Songnen grasslands was characterized by steppes similar to those of the present landscape. Local vegetation of the peatlands was typically dominated by sedges, which is also similar to present-day conditions.

From 7300 cal BP to 6000 cal BP, the Dabusu peatlands had a high-water level. The water level lowered rapidly between 6000 and 5100 cal BP. The period 5100-910 cal BP was characterized by a relatively low level, followed by a slight rise after 910 cal BP.

Comparing these results with regional paleoclimate records indicates that EASM circulation was the main driving force controlling both paleovegetation dynamics in the Songnen grasslands and hydrological variations of the Dabusu peatlands. IRD events were less significant than EASM variations in influencing both regional vegetation changes and the water-level fluctuations within the Dabusu peatlands.

ACKNOWLEDGMENTS

This work was financially supported by the National Nature Science Foundation of China (awards 41971100, 41771214 , 41471164), and the Natural Science Foundation of Jilin Province (award

20180101088JC), Jilin Songnen Grassland Ecosystem National Observation and Research Station,Program of Introducing Talents of Discipline to Universities (B16011).

Declaration of interests

The authors declare that they have no known competing financial interests or personal relationships that could have appeared to influence the work reported in this paper.

The authors declare the following financial interests/personal relationships which may be considered as potential competing interests:

References

Alexandre, A., Meunier, J.D., Lézine, A.M., Vincens, A., Schwartz, D., 1997. Phytoliths: Indicators of grassland dynamics during the late Holocene in intertropical Africa. Palaeogeography, Palaeoclimatology, Palaeoecology, 136, 213-229.

An, Z., 2000. The history and variability of the East Asian paleomonsoon climate. Quaternary Science Reviews, 19, 171-187.

Barboni, D., Bonnefille, R., Alexandre, A., Meunier, J. D., 1999. Phytoliths as paleoenvironmental indicators, West Side Middle Awash Valley, Ethiopia. Palaeogeography, Palaeoclimatology, Palaeoecology, 152, 87-100.

Berger, A., Loutre, M. F., Kaspar, F., Lorenz, S. J., 2007. Insolation during interglacial. Developments in Quaternary Sciences, 7, 13-27.

Bond, G. C., Kromer, B., Beer, J., Muscheler, R.., Evans, M., N., Showers, W., Hoffmann, S., Lotti-Bond, R., Hajdas, I., Bonani, G., 2001. Persistent solar influence on North Atlantic climate during the Holocene. Science, 294 (5549), 2130-2136.

Boyd, M., 2005. Phytoliths as paleoenvironmental indicators in a dune field on the northern Great Plains. Journal of Arid Environments, 61, 357-375.

Brewer, S., Giesecke, T., Davis, B., Finsinger, W., Wolters, S., Binney, H., Beaulieu, J., Fyfe, R., Gil-Romera, G., Kühl, N., Kuneˇs, P., Leydet, M., Bradshaw, R.H., 2017. Late-glacial and Holocene European pollen data. Journal of Maps. 13, 921-928.

Cao, Z., Hu, K., Zhang, Y., Jie, D., Zhao, L., 2005. Grains size distribution and wind erosion possibilities of surface sediments in Horqin sandland. Journal of Desert Research, 25 (1):16-19 (in Chinese).

Chambers, F., M., Beilman, D., W., Yu, Z., 2011. Methods for determining peat humification and for quantifying peat bulk density, organic matter and carbon content for palaeostudies of climate and peatland carbon dynamics. Mires and Peat, 7 (7), 1-10.

Chen, C., Tao, S., Zhao, W., Jin, M., Wang, Z., Li, H., Ren, H., Li, G., 2021. Holocene lake level, vegetation, and climate at the East Asian summer monsoon margin: A record from the Lake Wulanhushao basin, southern Inner Mongolia. Palaeogeography, Palaeoclimatology, Palaeoecology, 561, 110051.

Chen, F., H., Yu, Z., C., Yang, M., L., Ito, E., Wang, S., M., Madsen, D., B., Huang, X., Zhao, Y., Sato, T., Birks, H., Boomer, I., Chen, J., An, C., Wubbemann, B., 2008. Holocene moisture evolution in arid central Asia and its out-of-phase relationship with Asian monsoon history. Quaternary Science Review, 27 (3-4), 351-364.

Chen, X., Bu, Z., Stevenson, M. A., Cao, Y., Zeng, L., Qin, B., 2016. Variations in diatom communities at genus and species levels in peatlands (central China) linked to microhabitats and environmental factors. Science of the Total Environment, 568, 137-146.

Cosford, J., Qing, H., Mattey, D., Eglinton, B., Zhang, M., 2009. Climatic and local effects on stalagmite $\delta^{13}C$ values at Lianhua Cave, China. Palaeogeography. Palaeoclimatology. Palaeoecology, 280, 235-244.

Cour, P., Zheng, Z., Duzer, D., Calleja, M., Yao, Z., 1999. Vegetational and climatic signifificance of modern pollen rain in northwestern Tibet. Review of Palaeobotany & Palynology, 104 (3-4), 183-204.

Dam, H., Mertens, A., Sinkeldam, J., A., 1994. Coded check list and ecological indicator values of freshwater diatoms from the Netherlands. Netherlands Journal of Aquatic Ecology, 28 (1), 117-133.

Denys, L., A., 1991. Check-list of the diatoms in the Holocene deposits of the Western Belgian coastal plain with a survey of their apparent ecological requirements. I. Introduction, ecological code and complete list. Geological Service of Belgium.

Dobie, P., 2001. Poverty and the Drylands. Environmental Policy Collection, University of North Texas.

Francke, A., Wagner, B., Leng, M. J., Rethemeyer, J., 2013. A late glacial to Holocene record of environmental change from Lake Dojran (Macedonia, Greece). Climate of the Past, 9 (1), 481-498.

Gao, F., Jia, J., Xia, D., Lu, C., Lu, H., Wang, Y., Liu, H., Ma, Y., Li, K., 2019. Asynchronous Holocene climate optimum across mid-latitude Asia. Palaeogeography, Palaeoclimatology, Palaeoecology, 518 (15), 206-214.

Giesecke, T., Brewer, S., 2018. Notes on the postglacial spread of abundant European tree taxa. Vegetation History and Archaeobotany. 27, 337-349.

Goudie, A.S., 2002. Great Warm Deserts of the World: Landscapes and Evolution. Oxford University Press, New York.

Grimm, E., 1987. CONISS: a FORTRAN 77 program for stratigraphically constrained cluster analysis by the method of incremental sum of squares. Computer and Geosciences, 13, 13-35.

Grimm, E.C., 1991. TILIA and TILIA-GRAPH. Illinois State Museum, Springfield.

Hargan, K.E., Rühland, K.M., Paterson, A.M., Finkelstein, S.A., Holmquist, J.R., MacDonald, G.M., Keller, W., Smol, J.P., 2015. The influence of water-table depth and pH on the spatial distribution of diatom species in peatlands of the Boreal Shield and Hudson Plains, Canada. Botany 93, 57-74.

Hofmann, M., H., 2005. Sedimentary record of glacial dynamics, lake level fluctuations, and tectonics: Late Pleistocene-Holocene structural and stratigraphic analysis of the Flathead Lake basin and the Mission Valley, Montana, United States America. University of Montana.

Horowitz, A., 1992. Palynology of Arid Lands. Amsterdam: Elsevier.

Huang, J., Ma, J., Guan, X., Li, Y., He, Y. 2019. Progress in Semi-arid Climate Change Studies in China. Advances in Atmospheric Sciences, 36, 922-937.

Huang, X., Zhou, G., Ma, Y., Xu, Q., Chen, F., 2010. Pollen distribution in large freshwater lake of arid region: a case study on the surface sediments from Bosten Lake, Xinjiang, China. Frontiers of Earth Science in China, 4 (2), 174-180.

Huang, X., Xiang, L., Lei, G., Sun, M., Qiu, M., Storozum, M., Huang, C., Munkhbayard, C., Demberele, O., Zhang, J., Zhang, J. W, Chen, J., Chen, X., Chen, F., 2021. Sedimentary Pediastrum record of middle–late Holocene temperature change and its impacts on early

human culture in the desert-oasis area of northwestern China. Quaternary Science Reviews, 265, 107054.

Huntley, B., 2010. European vegetation history: Palaeovegetation maps from pollen data − 13 000 yr BP to present. Journal of Quaternary Science, 5, 103-122.

Jia, X., Lee, H. F., Zhang, W., Wang, L., Sun, Y., Zhao, Z., Yi, S., Huang, W., Lu, H., 2016. Human-environment interactions within the West Liao River basin in Northeastern China during the Holocene Optimum. Quaternary International, 426, 10-17.

Jiang, Q., Hao, Q., Peng, S., Qiao, Y., 2020. Grain-size evidence for the transport pathway of the Xiashu loess in northern subtropical China and its linkage with fluvial systems. Aeolian Research, 46, 100613.

Jie, D. M., Fu, L., J., Min, L. Z., Leng, X., T., Wang, S.Z., Zhang, G.R., 2001. Carbonate content of sedimentary core and Holocene lake-level fluctuation of Dabusu lake. Marine Geology & Quaternary Geology, 33 (2), 178-192 (in Chinese).

Kassambara, A., Mundt, F., 2019. Rpackage “factoextra”: extract and visualize the results of multivariate data analyses (version 1. 0. 6).Available from. http://www.sthda.com/english/rpkgs/factoextra.

Khon, V. C., Wang, Y. V., Krebs-Kanzow, U., Kaplan, J. O., Schneider, R. R., Schneider, B., 2014. Climate and CO_2 effects on the vegetation of southern tropical Africa over the last 37,000 years. Earth and Planetary Science Letters, 403, 407-417.

Li, B., 1994. Analysis of climatic factors on desertification of Songnen Sandy Land and its developmental trend in the future. Journal of Northeast Normal University (Natural Science Edition), 2, 94 – 99 (in Chinese).

Li, F., Sun, J., Zhao, Y., Guo, X., Zhao, W., Zhang, K., 2010. Ecological significance of common pollen ratios: a review. Frontiers of Earth Science in China, 4 (3), 253-258.

Li, J., Xu, Q., Gaillard-Lemdahl, M. J., Seppä, H., Li, Y., Hun, L., Li, M., 2013. Modern pollen and land-use relationships in the Taihang mountains, Hebei province, northern China—a first step towards quantitative reconstruction of human-induced land cover changes. Vegetation history & archaeobotany, 22 (6), 463-477.

Li, M., Xu, Q., Zhang, S., Li, Y., Ding, W., Li, J., 2015. Indicator pollen taxa of human-induced and natural vegetation in Northern China. The Holocene, 25 (4), 686-701.

Li, N., Sack, D., Gao, G., Liu, L., Li, D., Yang, X., Jie, D., Liu, H., Shi, J., Leng, C., 2018. Holocene Artermisia-Chenopodiaceae dominated grasslands in North China: Real or imagination? The Holocene, 28 (5), 834-841.

Li, N., 2020. Response of Vegetation Dynamics to Climate Change since the Younger Dryas in the Longgang Region, Northeastern China. Northeast normal university.

Li, N., Xie, M., Sack, D., Dubois, N., Yang, X., Gao, G., Li, D., Liu, L., Liu, H., Leng, C., Wang, J., Liu, B., Jie, D., 2021. Continuous aridification since the mid-Holocene as the main cause of C3/C4 dynamics in the grasslands of northeastern China. European Journal of Soil Science, 72 (1), 356-371.

Li, Q., 1991. A primary study on the historical change of Songnen Sandy Land. Chinese Science Bulletin, 36, 487-489.

Li, W.Y., Yao, Z.J., 1990. A study on the quantitative relationship between Pinus pollen in surface sample and Pinus vegetation. Acta Botanica Sinica, 32 (12), 943-950 (in Chinese).

Li, X., Zhao, C., Zhou, X., 2019. Vegetation pattern of Northeast China during the special periods since the Last Glacial Maximum. Science China Earth Sciences, 62, 1224-1240 (in Chinese).

Li, Y., Lu, J., 1996. The spore-pollen records of vegetation and climate history in Songnen sandy land since epipleistocene. Journal of Desert Research, 16(4), 338-344 (in Chinese).

Li, Y., Xu, Q., Yang, X., Zheng, Z., 2005a. Pollen assemblages of major steppe communities in China. Acta ecologica Sinica, 25 (3), 556-564 (in Chinese).

Li, Y.C., Xu, Q.H., Xiao, J.L., Yang, X., 2005b. Indication of some major pollen taxa in surface samples to their parent plants of forest in northern China. Quaternary Sciences, 25 (5), 598-608 (in Chinese).

Li, Z., Wang, Y., Herzschuh, U., Cao, X., Ni, J., Zhao, Y., 2021. Pollen-based mapping of Holocene vegetation on the Qinghai-Tibetan Plateau in response to climate change. Palaeogeography, Palaeoclimatology, Palaeoecology, 573, 110412.

Li, Z., Lv, J., 2001. Geomorphology, deposition and lake Evolution of Dabusu Lake, Northeastern China. Lake Science, 13 (2), 103-110.

Li, Z., Gao, Y., Han, L., 2017. Holocene vegetation signals in the Alashan Desert of northwest China revealed by lipid molecular proxies from calcareous root tubes. Quaternary Research, 88 (1), 60-70.

Liu, H.Y., Wang, Y., Tian, Y.H., Zhu, J.L., Wang, H.Y., 2006. Climatic and anthropogenic control of surface pollen assemblages in East Asian steppes. Review of Palaeobotany & Palynology, 138 (3–4), 281-289.

Liu, W., Feng, X., Ning, Y., Zhang, Q., Cao, Y., An, Z., 2005. $\delta^{13}C$ variation of C3 and C4 plants across an Asian monsoon rainfall gradient in arid northwestern China. Global Change Biology, 11, 1094-1100.

Ma, R., Duan, H., Hu, C., Feng, X., Li, A., Ju, W., Jiang, J., Yang, G., 2010. A half-century of changes in China's lakes: Global warming or human influence? Geophysical Research Letters. 37, L24106.

Mancini, M.V., 2009. Holocene vegetation and climate changes from a peat pollen record of the forest-steppe ecotone, Southwest of Patagonia (Argentina). Quaternary Science Review, 28, 1490-1497.

Marquer, L., Gaillard, M.J., Sugita, J., Poska, A., Trondman, A.K., Mazier, F., Nielsen, A.B., Fyfe, R.M., Jönsson, A.M., Smith, B., Kaplan, J.O., Alenius, T., Birks, J.B., Bjune, A.E., Christiansen, J., Dodson, J., Edwards, K.J., Giesecke, T., Herzschuh, U., Kangur, M., Koff, T., Latałowa, M., Lechterbeck, J., Olofsson, J., Seppä, H., 2017. Quantifying the effects of land use and climate on Holocene vegetation in Europe. Quaternary Science Reviews, 171, 20-37.

Nelson, D.M., Hu, F.S., Tian, J., Stefanova, I., Brown, T.A., 2004. Response of C3 and C4 plants to middle-Holocene climatic variation near the prairie-forest ecotone of Minnesota. Proceedings of the National Academy of Sciences of the United States of America, 101, 562-567.

Owen, R.B., Renaut, R.W., Jones, B., 2008. Geothermal diatoms: a comparative study of floras in hot spring systems of Iceland, New Zealand, and Kenya. Hydrobiologia, 610 (1), 175-192.

Pachauri, R.K., Allen, M.R., Barros, V.R., Broome, J., Cramer, W., Christ, R., Church,J., Clarke L., Qin, D., Dasqupta, P., Dubash, N., Edenhofer, O., Elgizouli, I., Field, C., Forster P., Friedlingstein, P., Fuglestvedt, J., Gomez-Echeverri, L., Hallegatte, S., HegerlShow G., Jiang, K., Cisneros, B., Kattsov, V., Lee, H., Mach, K., Marotzke, J., Mastrandrea, D., Meyer, L., Minx, J., Mulugetta, Y., Brien, K., Oppenheimer M., Pereira, J., Pichs-Madruga, R., Plattner, G., Pörtner, H., Power, S., Preston, B., Ravindranath, N., Reisinger, A., Riahi, K., Rusticucci, M., Scholes, R., Seyboth, K., Sokona, Y., Stavins, R., Stocker, T., Tschakert, P., Vuuren, D.,

Van Ypserle, J. P., 2014. Climate change 2014: synthesis report. Contribution of Working Groups I, II and III to the fifth assessment report of the Intergovernmental Panel on Climate Change (p. 151). IPCC.

Pribyl, D.,W., 2010. A critical review of the convencional SOC to SOM conversion factor. Geoderma, 156, 75-83.

Pye, K., 1987. Aeolian Dust and Dust Deposits. Academic Press, London.

Qiu, S., Li, Q., Xia, Y., 1992. Paleosols of sandy lands and environmental changes in the western plain of Northeast China during Holocene. Quaternary Science, 3, 224–232 (in Chinese).

Reynolds, J.F., Smith, D., Lambin, E., Turner, B., Mortimore, M., Batterbury, S., Downing, T., Dowlatabadi, H., Fernandez, R., Herrick, J., Huber-Sannwald, E., Jiang, H., Leemans, R., Lynam, T., Maestre, F., Ayarza, M., Walker, B., 2007. Global desertification: building a science for dryland development. Science, 316 (5826), 847-851.

Serieyssola, K., 2012. Diatoms of Europe: Diatoms of the European Inland Waters and Comparable Habitats. Diatom Research, 27 (2), 103-108.

Shao, Y., 2008. Physics and Modelling of Wind Erosion. Springer Science & Business Media.

Shen, Y., Zhang, C., Li, Q., Jia, W., Li, J., Tian, J., 2016. Grain-Size characteristics of surface sediments in the eastern regions of China. Journal of Desert Research, 36 (1), 151-156 (in Chinese).

Sjögren, P., Willem, O.K., Jacqueline, F.L., 2015. Pollen dispersal properties of Poaceae and Cyperaceae: first estimates of their absolute pollen productivities. Review of Palaeobotany and Palynology, 216, 123-131.

Stockner, J.G., 1967. Observations of thermophilic algal communities in Mount Rainier and Yellowstone National Parks. Limnology and Oceanography, 12, 13–17.

Strömberg, C.A., Dunn, R.E., Crifò, C., Harris, E.B., 2018. Phytoliths in paleoecology: analytical considerations, current use, and future directions. Methods in Paleoecology, Vertebrate Paleobiology and Paleoanthropology. Springer, Cham.

Stuut, J.B., Smalley, I., O'Hara-Dhand, K., 2009. Aeolian dust in Europe: African sources and European deposits. Quaternary International, 198, 234-245.

Tao, S., Fang, J., Zhao, X., Zhao, S., Shen, H., Hu, H., Tang, Z., Wang, Z., Guo, Q., 2015. Rapid loss of lakes on the Mongolian Plateau. Proceedings of the National Academy of Sciences of the United States of America.112 (7), 2281-2286.

Tooth, S., 2009. Arid geomorphology: emerging research themes and new frontiers. Progress in Physical Geography, 33, 251-287.

Vis, G.J., Bohncke, S.J.P., Schneider, H., Kasse, C., Coenraads-Nederveen, S., Zuurbier, K., Rozema, J., 2010. Holocene flooding history of the Lower Tagus Valley (Portugal). Journal of Quaternary Science, 25 (8), 1222-1238.

Wang, P., Wang, B., Cheng, H., Fasullo, J., Guo, Z., Kiefer, T., Liu, Z., 2017. The global monsoon across time scales: mechanisms and outstanding issues. Earth Science Reviews. 174, 84-121.

Weltje, G.J., Prins, M.A., 2007. Genetically meaningful decomposition of grain-size distributions. Sedimentary Geology, 202, 409-424.

Wu, J., Wang, Y., Dong, J., 2011. Changes in East Asian summer monsoon during the Holocene recorded by stalagmite $\delta^{18}O$ records from Liaoning Province. Quaternary Science, 31 (6), 990-998 (in Chinese).

Xiao, J., Fan, J., Zhou, L., Zhai, D., Wen, R., Qin, X., 2013. A model for linking grain-size component to lake level status of a modern clastic lake. Journal of Asian Earth Science, 69, 149-158.

Xiao, R., 1995. Geographical location and principle regional characteristics of desertification-prone lands of the Songnen Sandy Land. In R. Xiao (Ed.), The Research on the Desertification of the Songnen Sandy Land in Northeast China. Northeast Normal University Press (in Chinese).

Xiao, Y., Xiang, L., Huang, X., Mills, K., Zhang, J., Chen, X., Li, Y., 2021. Moisture Changes in the Northern Xinjiang Basin Over the Past 2400 years as Documented in Pollen Records of Jili Lake. Frontiers in Earth Science, 9, 741992.

Xu, D., Lu, H., Chu, G., Liu, L., Shen, C., Li, F., Wang, C., Wu, N., 2019. Synchronous 500-year oscillations of monsoon climate and human activity in Northeast Asia. Nature Communications 10, 4105

Xu, Q., Li, Y. C., Yang, X., Zheng, Z., 2007a. Quantitative relationship between pollen and vegetation in northern China. Science in China Series D: Earth Sciences, 50 (4), 582-599.

Xu, Q., Li, Y., Yang, X.L., Zheng, Z.H., 2007b. Quantitative relationship between several main pollen types and vegetation in northern China. Science in China press, 37 (2), 192-205.

Yan, S., 1991. The characteristics of Quaternary sporo-pollen assemblage and the vegetation succession in Xinjiang. Arid Land Geography, 14, 1-9 (in Chinese)

Yang, X., Scuderi, L., Paillou, P., Liu, Z., Li, H., Ren, X., 2011. Quaternary environmental changes in the drylands of China–a critical review. Quaternary Science Reviews, 30 (23-24), 3219-3233.

Yang,Y., Ma, X., Wang, L., Fu, X., Zhang, J., 2016. Evaluation of three methods used in carbonate content determination for lacustrine sediments. Lake Science, 28 (4), 917-924 (in Chinese).

Yu, G., Prentice, I.C., Harrison, S.P., Sun, X.J., 1998. Pollen based biome reconstructions for China at 0 and 6000 years. Journal of Biogeography, 25 (6), 1055-1069.

Zanon, M., Davis, B.A.S., Marquer, L., Brewer, S., Kaplan, J.O., 2018. European forest cover during the past 12,000 years: a palynological reconstruction based on modern analogs and remote sensing. Frontiers in Plant Science, 9, 253.

Zhang, G., Liu, H., Jie, D., Liu, Y., Meng, M., Wang J., Gao, G., Li, D., Li, N., Niu, H., Leng, C., 2020. Analyzing differences of topsoil organic matter and grain size of different types of dunes in Horqin. Ecology and Environmental Sciences, 29 (11), 2223-2230.

Zhang, L., Wei, B., Ge, Q., Hao, M., Fu, H., Zhang, W., Jiang, Z., 2012. Relationship between productivity and plant functional traits along successive recovery stages in an alpine meadow. Acta Pratacurae Sinica, 21 (6), 235-241.

Zhang, J.W., Chen, F. H., Holmes, J. A., Li, H., Guo, X. Y., Wang, J. L., Li, S., Lv, Y. B., Zhao, Y., Qiang, M. R., 2011. Holocene monsoon climate documented by oxygen and carbon isotopes from lake sediments and peat bogs in China: a review and synthesis. Quaternary Science Review, 30, 1973-1987.

Zhang, W.Q., Chen, J. S., Jiang, S,.K., Xu, Y., 2017. Study of recharge of Dabusu lake in Songnen plain based on isotopic and hydrochemical analysis. Water Resources Protection, 33 (1), 9-16.

Zhang, Z., Zhao, M., Lu, H., Faiia, A.M., 2003. Lower temperature as the main cause of C4 plant declines during the glacial periods on the Chinese Loess Plateau. Earth and Planetary Science Letters, 214, 467-481.

Zhang, Z., Xing, W., Lv, X., Wang, G., 2014. The grain-size depositional process in wetlands of the Sanjiang Plain and its links with the East Asian monsoon variations during the Holocene. Quaternary international, 349, 245-251.

Zhang, Z., Yao, Q., Xu, Q., Jiang, M., Zhu, T., 2021. Hydrological and palynological evidence of wetland evolution on the Sanjiang Plain (NE China) in response to the Holocene East Asia summer monsoon. CATENA, 203, 105332.

Zhao, B., 2014. Archaeological research in northeast China. Science Press.

Zhao, Y., Yu, Z., Chen, F., Liu, X., Ito, E., 2008. Sensitive response of desert vegetation to moisture change based on a near-annual resolution pollen record from Gahai Lake in the Qaidam Basin, northwest China. Global and Planetary Change, 62 (1-2), 107-114.

Zhao, Y., Yu, Z., Chen, F., Zhang, J., Yang, B., 2009. Vegetation response to Holocene climate change in monsoon-influenced region of China. Earth-Science Reviews, 97, 242-256.

Zhao, Y., Herzschuh, U., 2009. Modern pollen representation of source vegetation in the Qaidam Basin and the surrounding mountains, north-eastern Tibetan Plateau. Vegetation History and Archaeobotany, 18 (3), 245-260

Zhao, Y., Yu, Z., 2012. Vegetation response to Holocene climate change in East Asian monsoon-margin region. Earth-Science Reviews, 113, 1-10.

Zhu, Z., Chen, Z., Wu, Z., Li, J., Li, B., Wu, G., 1981. Study on the geomorphology of wind-drift sands in the Taklamakan Desert. Science Press, Beijing (in Chinese).

Zuo, X.A., Knops, J.M.H., Zhao, X.Y., Zhao, H,.L., Li, Y.Q., Guo, Y.R., 2011. A positive correlation between plant diversity and productivity is indirectly caused by environmental factors driving spatial pattern of vegetation composition in semiarid sandy grassland. Biogeosciences Discussions, 8 (6), 11795–11825.

FIGURES

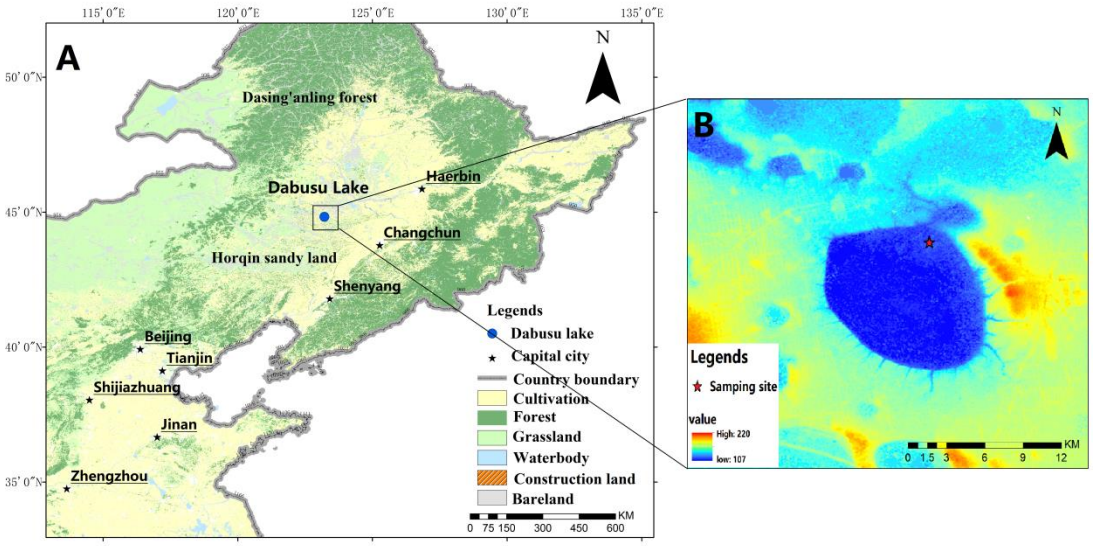

Fig. 1. A. Location of the Dabusu peatlands in northeastern China. **B.** Lake Dabusu and its surroundings. The sediment coring site is marked with a red star.

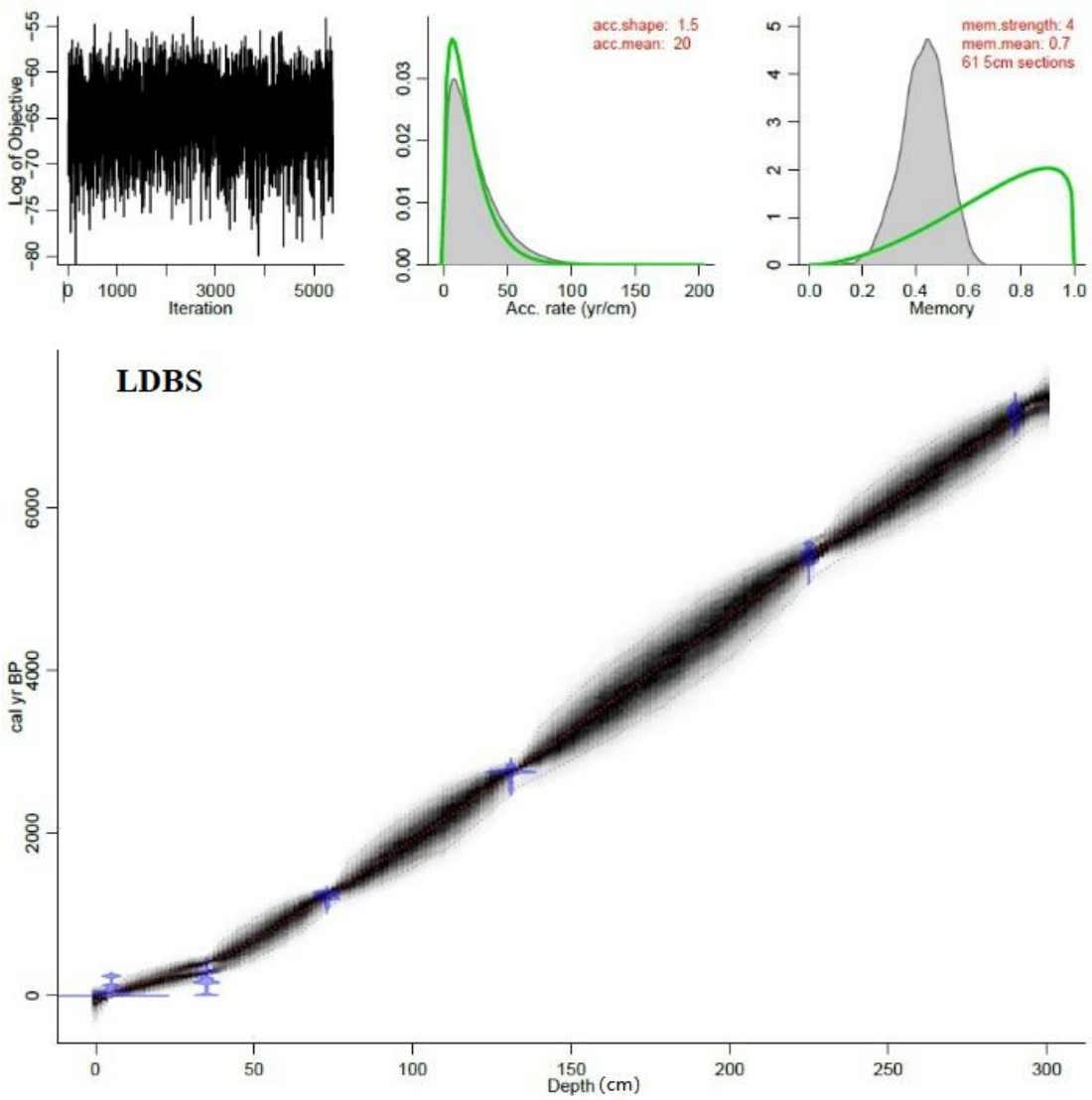

Fig. 2. The 'Bacon' age-depth model for Dabusu peat profile based on six calibrated radiocarbon dates (obtained from bulk organic matter and plant residues, see Table 1). The LDBS-6 date was excluded for establishing the age-depth model due to a chronological inversion.

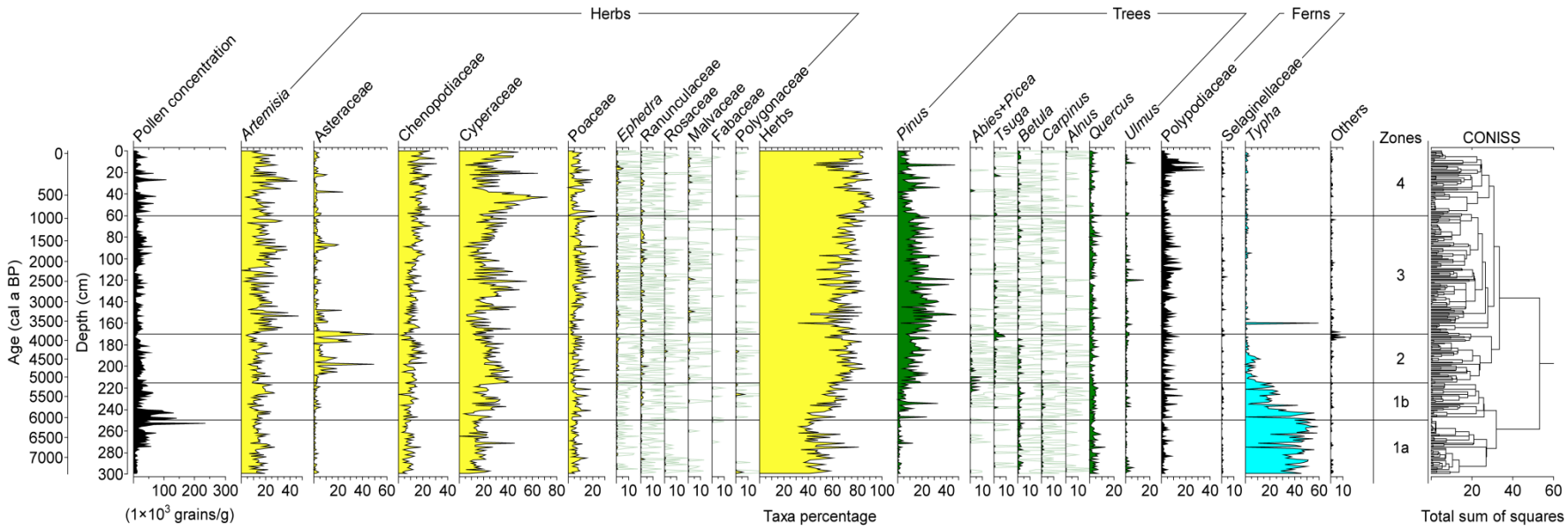
Herbs
Trees
Ferns
Pollen concentration
Artemisia
Asteraceae
Chenopodiaceae
Cyperaceae
Poaceae
Ephedra
Ranunculaceae
Rosaceae
Malvaceae
Fabaceae
Polygonaceae
Herbs
Pinus
Abies+Picea
Tsuga
Betula
Carpinus
Alnus
Quercus
Ulmus
Polypodiaceae
Selaginellaceae
Typha
Others
Zones
CONISS
Age (cal a BP)
Depth (cm)
(1×10³ grains/g)
Taxa percentage
Total sum of squares
4
3
2
1b
1a

Fig. 3. Pollen percentages and pollen concentrations of the Dabusu peat sequence, plotted against depth (cm) and year (cal BP). The results of the CONISS analysis (based on the total sum of squares) appear on the right. Horizontal lines mark the pollen zones. A 20-fold exaggeration was used for taxa with low abundances (< 5%; shown in light green),. Pollen types from herbs and trees are colored red and green, respectively.

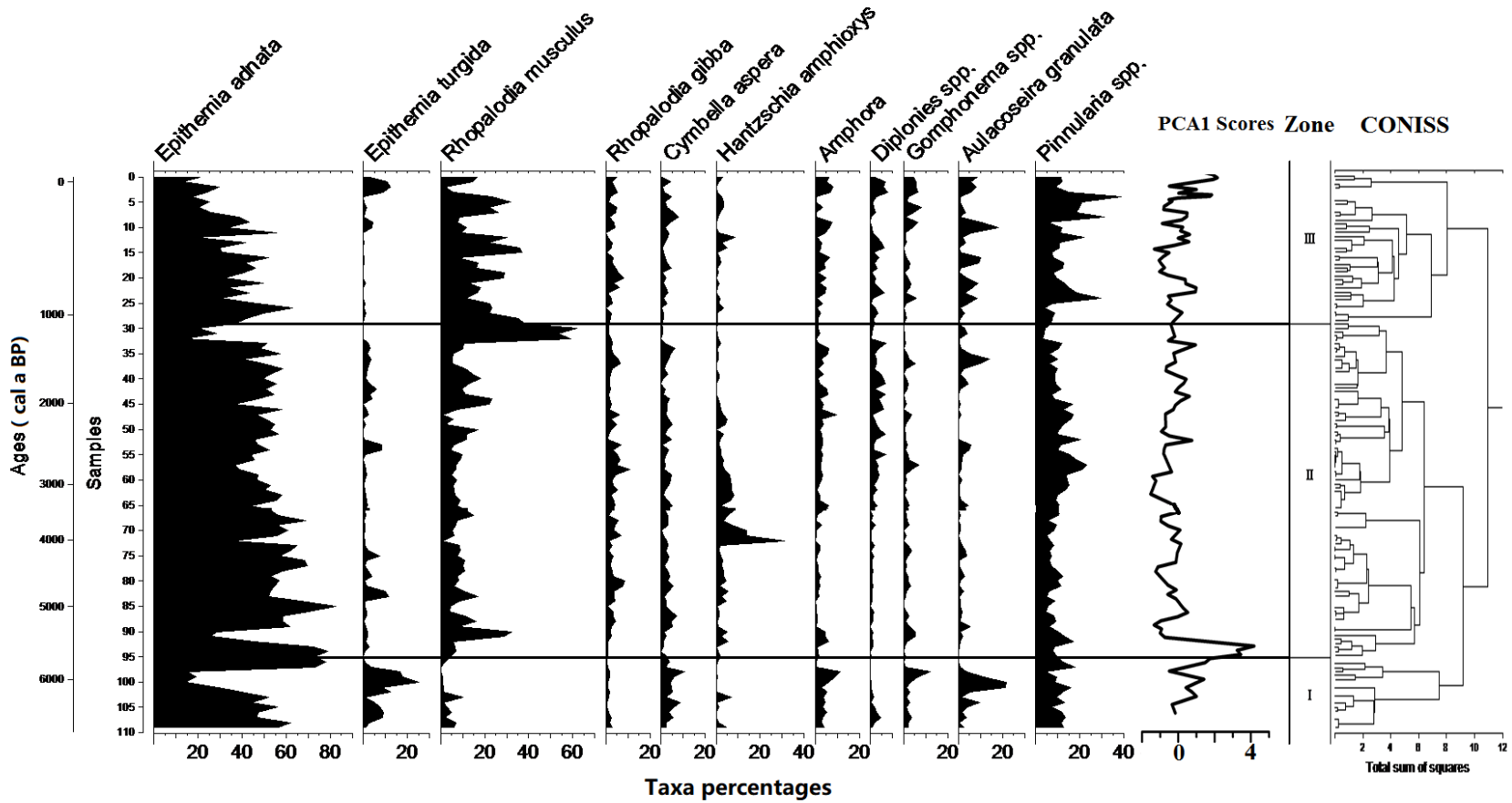
Epithemia adnata
Epithemia turgida
Rhopalodia musculus
Rhopalodia gibba
Cymbella aspera
Hantzschia amphioxys
Amphora
Diplonies spp.
Gomphonema spp.
Aulacoseira granulata
Pinnularia spp.
PCA1 Scores
Zone
CONISS
Ages (cal a BP)
Samples
Taxa percentages
Total sum of squares
I
II
III

Fig. 4. Diatom stratigraphy from Lake Dabusu. Relative abundance (%) of the most abundant species. Only the species with a mean percentage above 2% are shown.

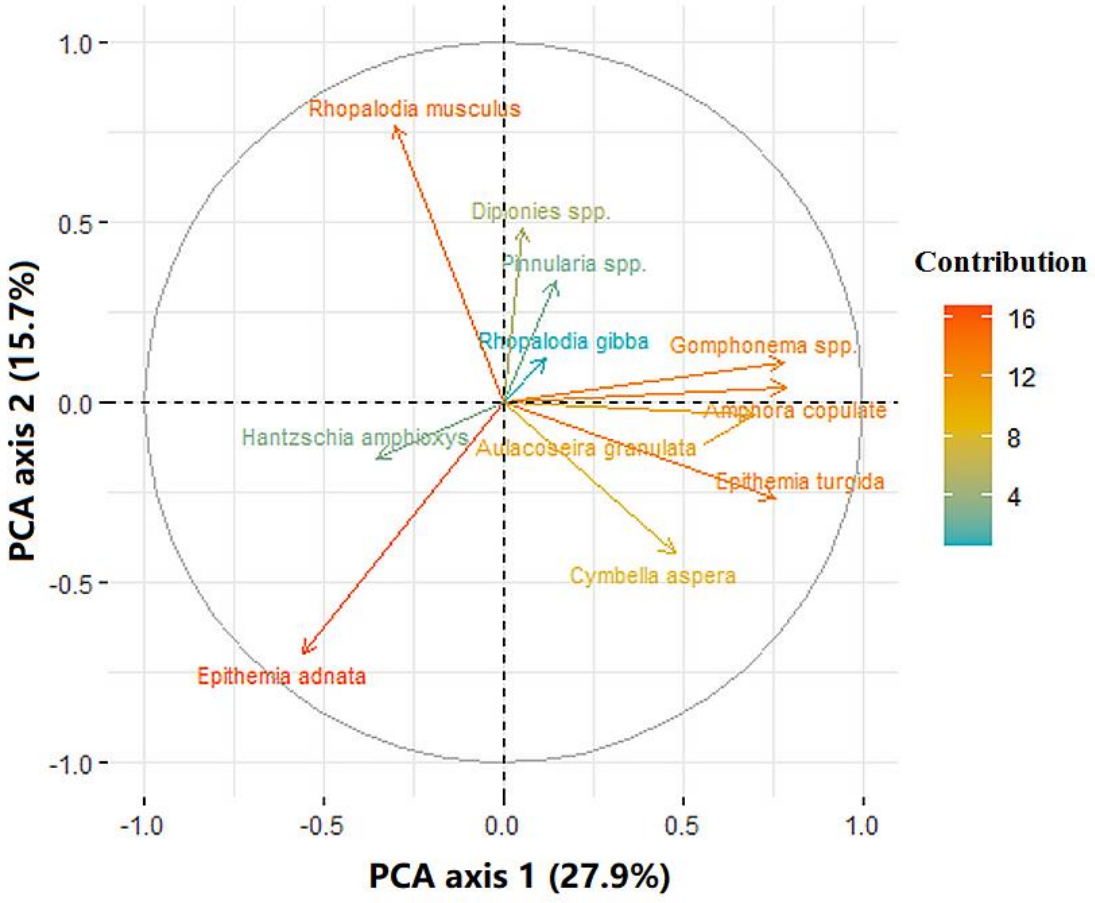

Fig.5. Principal component analysis (PCA) of diatom variables. Contribution bar (on right) highlights the most significant variables that explain the variations by the principal components.

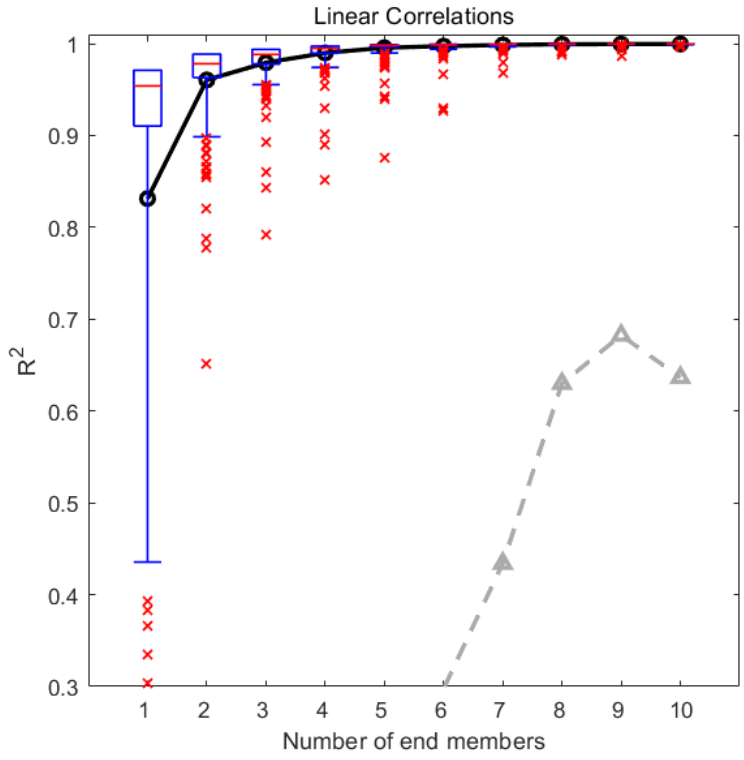

Fig.6. Plots of the variance of the entire dataset of Dabusu peat core samples explained by different numbers of end members.

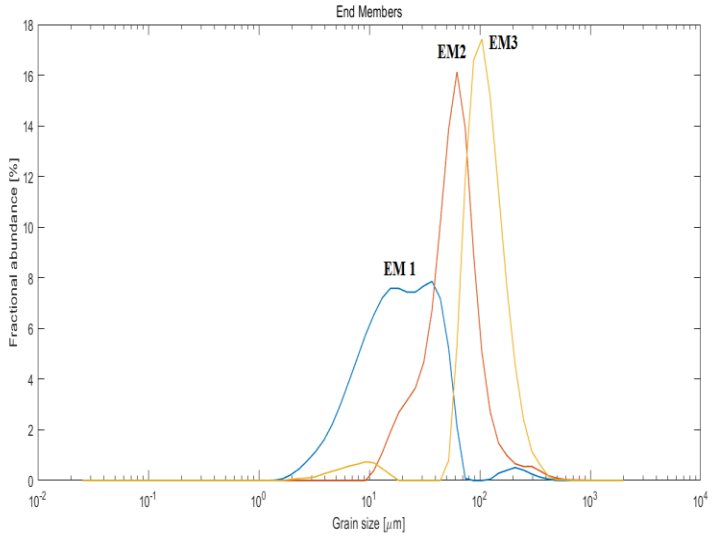

Fig.7. Grain-size distributions for the three end members (EM 1-3).

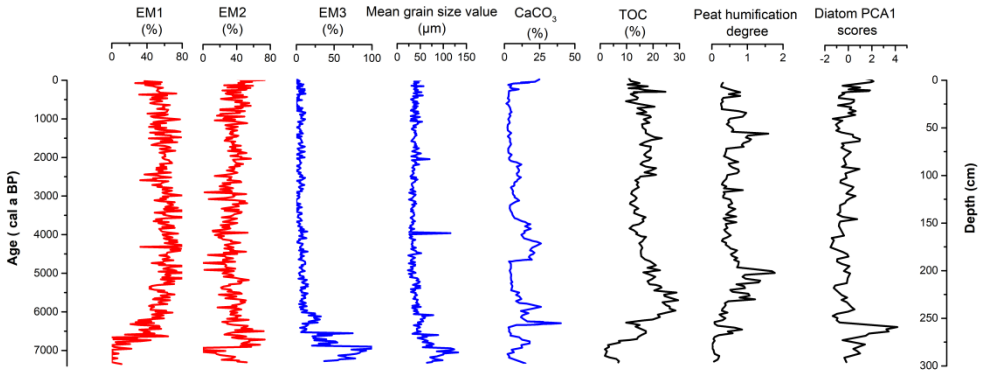

Fig. 8. Summary diagram showing end-member analysis, variations in mean grain size, total organic carbon (TOC) and carbonate ($CaCO_3$) content, peat humification degree and PCA 1 scores for diatoms (yellow fill is used to clearly indicate the consistent changes of the curves).

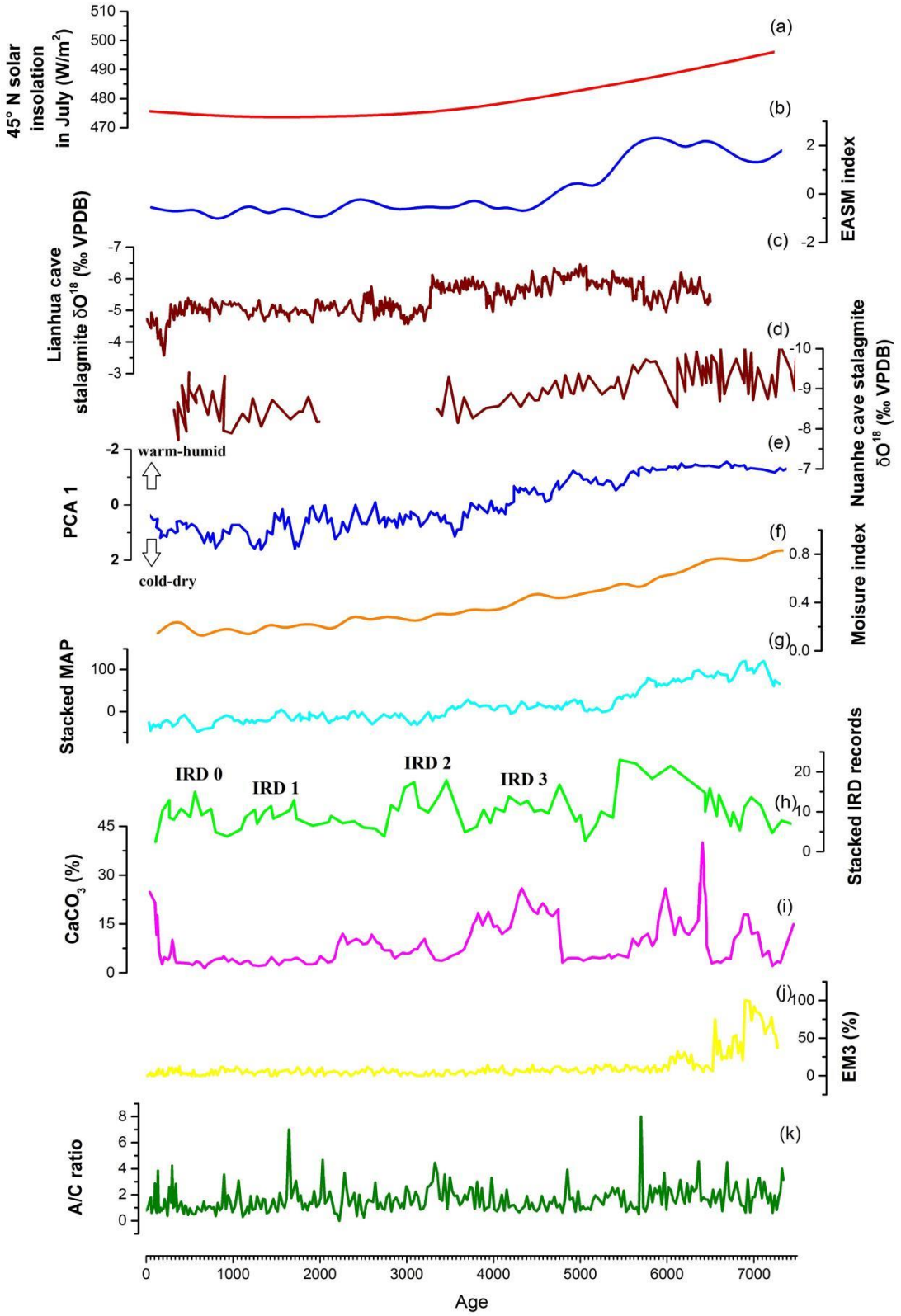
45° N solar insolation in July (W/m²)
510
500
490
480
470
(a)
(b)
EASM index
2
0
-2
(c)
Lianhua cave stalagmite δO¹⁸ (‰ VPDB)
-7
-6
-5
-4
-3
(d)
Nuanhe cave stalagmite δO¹⁸ (‰ VPDB)
-10
-9
-8
-7
(e)
PCA 1
-2
0
2
warm-humid
cold-dry
(f)
Moisure index
0.8
0.4
0.0
(g)
Stacked MAP
100
0
IRD 0
IRD 1
IRD 2
IRD 3
(h)
Stacked IRD records
20
10
0
CaCO₃ (%)
45
30
15
0
(i)
(j)
EM3 (%)
100
50
0
A/C ratio
8
6
4
2
0
(k)
0
1000
2000
3000
4000
5000
6000
7000
Age

Fig. 9. Holocene environmental context of the Dabusu peatlands compared to the regional and global climate trends. (a) North hemisphere 45° solar irradiation (Berger et al., 2007); (b) The EASM index by Chen et al., 2008; (c) The stalagmite $\delta^{18}O$ records from Lianhua cave, northern China (Cosford et al., 2009); (d) The stalagmite $\delta^{18}O$ records from Nuanhe cave, northeastern China (Wu et al., 2011); (e) Climate moisture based on the PCA 1 score calculated from pollen records of lake Xiaolongwan in northeastern China (Xu et al., 2019); (f) Synthesized moisture index based on $\delta 18O_{carb}$ for East Asian summer monsoon regions (Zhang et al., 2011); (g) The stacked MAP curve was calculated from the climate records quantitatively reconstructed by pollen records from five lakes in East Asian summer monsoon regions (Zhang et al., 2021). (h) Holocene stacked IRD (ice rafted debris) events in North Atlantic (Bond et al., 2001); (i) $CaCO_3$ contents of Dabusu peatlands (this study); (j) Grain-size end members EM3 of Dabusu peatlands (this study); (k) A/C ratios calculated based on pollen percentages from this study.

TABLES

Table 1. Radiocarbon dates obtained from the Dabusu peat profile.

Core no.	Depth (cm)	Lab.code	Material	AMS ^{14}C yr BP	Uncertainty	2σ-range calibrations (cal. a BP) with Probability	Median age, cal. Yr BP
LDBS-1	35	NENUR 10479	Plant residues	215	35	135-225 (50.3%)	190
LDBS-2	73	NENUR 10480	Plant residues	1300	40	1170-1300 (90.9%)	1225
LDBS-3	131	NENUR 10481	Bulk organic matter	2625	40	2705-2800 (87.8%)	2750
LDBS-4	195	NENUR 10483	Bulk organic matter	5030	50	5655-5905 (93.4%)	5785
LDBS-5	225	NENUR 10484	Plant residues	4675	50	5310-5485 (85.7%)	5405
LDBS-6	258	NENUR 10485	Bulk organic matter	6320	60	7155-7365 (85.1%)	7240
LDBS-7	290	NENUR 10486	Bulk organic matter	6260	60	7145-7351 (60.3%)	7180

Highlights

- Steppes, dry-steppes, forest-steppes, dry steppes, and steppes have successively dominated the Songnen grasslands since the mid-Holocene.
- After experiencing the highest water level period in the early Mid-Holocene, Dabusu peatlands had a relatively low water level after 6000 cal BP interspersed by two relatively high water level periods: 5100-4000 cal BP and 910-the present cal BP.
- EASM circulations might be the main driving forces controlling the regional paleovegetation dynamics and hydrological variations.